Stem Cell Research 25 (2017) 61–71

Contents lists available at ScienceDirect

Stem Cell Research

journal homepage: www.elsevier.com/locate/scr

Lung regeneration after toxic injury is improved in absence of dioxin receptor

Antonio Morales-Hernández [a], Ana Nacarino-Palma [b], Nuria Moreno-Marín [b], Eva Barrasa [b], Beroé Paniagua-Quiñones [b], Inmaculada Catalina-Fernández [c], Alberto Alvarez-Barrientos [d], Xosé R. Bustelo [e], Jaime M. Merino [b,*], Pedro M. Fernández-Salguero [b,*]

[a] St. Jude Children's Research Hospital, Memphis, TN, USA
[b] Departamento de Bioquímica y Biología Molecular, Facultad de Ciencias, Universidad de Extremadura, 06071 Badajoz, Spain
[c] Servicio de Anatomía Patológica, Hospital Universitario Infanta Cristina, 06071 Badajoz, Spain
[d] Servicio de Técnicas Aplicadas a las Biociencias (STAB), Universidad de Extremadura, Badajoz, Spain
[e] Centro de Investigación del Cáncer and CIBERONC, CSIC-Universidad de Salamanca, 37007 Salamanca, Spain

ARTICLE INFO

Article history:
Received 22 May 2017
Received in revised form 7 August 2017
Accepted 9 October 2017
Available online 12 October 2017

Keywords:
Dioxin receptor
Liver and lung regeneration
Pluripotency
Stemness

ABSTRACT

Recent experimental evidences from cellular systems and from mammalian and non-mammalian animal models highlight novel functions for the aryl hydrocarbon/dioxin receptor (AhR) in maintaining cell differentiation and tissue homeostasis. Notably, AhR depletion stimulates an undifferentiated and pluripotent phenotype likely associated to a mesenchymal transition in epithelial cells and to increased primary tumorigenesis and metastasis in melanoma. In this work, we have used a lung model of epithelial regeneration to investigate whether AhR regulates proper tissue repair by adjusting the expansion of undifferentiated stem-like cells. AhR-null mice developed a faster and more efficient repair of the lung bronchiolar epithelium upon naphthalene injury that required increased cell proliferation and the earlier activation of stem-like Clara, Basal and neuroepithelial cells precursors. Increased basal content in multipotent Sca1^{+}/CD31^{-}/CD4^{-} cells and in cells expressing pluripotency factors NANOG and OCT4 could also improve re-epithelialization in AhR-null lungs. The reduced response of AhR-deficient lungs to Sonic Hedgehog (*Shh*) repression shortly after injury may also help their improved bronchiolar epithelium repair. These results support a role for AhR in the regenerative response against toxins, and open the possibility of modulating its activation level to favor recovery from lesions caused by environmental contaminants.

1. Introduction

Cell replacement and tissue regeneration under physiological conditions are rare events in most mammalian tissues with the exception of the immune system, skin epithelium and the lining of the gastrointestinal tract. However, several organs are capable of triggering a regenerative response after acute exposure to harmful agents. Specifically, lung and liver can replenish dead cells and restore tissue architecture and function from the activation of undifferentiated and differentiated precursors (Eisenhauer et al., 2013; Kotton and Morrisey, 2014; Leeman et al., 2014; Taub, 2004).

In the bronchiolar epithelium of the lung, cell tracing experiments have revealed the existence of Basal, Clara and type II alveolar stem-like cells whose differentiation give rise to ciliated and Goblet cells (Volckaert and De Langhe, 2014). In fact, Basal cells are considered stem progenitors able to generate Clara and ciliated cells in the proximal epithelium (Hong et al., 2004a,b, Rock et al., 2011, Rock et al., 2009) whereas Clara cells can either auto-renew or produce ciliated cells in the bronchus. Under homeostatic conditions, cells of neuroepithelial origin have also auto-renewing potential although their ability to make other cell types is limited (Song et al., 2012). Lung exposure to the toxic compound naphthalene (NPH) leads to a selective and massive destruction of Clara cells despite the appearance of an small pool of resistant cells that significantly contribute to regenerate the damaged bronchiolar epithelium (Giangreco et al., 2009; Giangreco et al., 2002; Rawlins and Hogan, 2006; Reynolds et al., 2000). Under injuring conditions, neuroepithelial cells can also differentiate to Clara and ciliated cells thus assisting in the renewal of the bronchioalveolar epithelium (Song et al., 2012).

Abbreviations: AhR, Aryl hydrocarbon (dioxin) receptor; CC10, Clara cell 10 protein; CCl_4, carbon tetrachloride; CK14, cytokeratin; CGRP, Calcitonin gene-related peptide; E-Cad, E-cadherin.

* Corresponding authors.
E-mail addresses: jmmerino@unex.es (J.M. Merino), pmfersal@unex.es (P.M. Fernández-Salguero).

https://doi.org/10.1016/j.scr.2017.10.009

The aryl hydrocarbon/dioxin receptor (AhR) has an increasing number of xenobiotic-dependent and xenobiotic-independent activities in the cell (Mulero-Navarro and Fernandez-Salguero, 2016; Pohjanvirta, 2012). From the homeostatic and physiological point of view, AhR has recognised roles in maintaining cell differentiation in the immune system (Esser and Rannug, 2015; Esser et al., 2009; Quintana et al., 2008; Veldhoen et al., 2008), gonads (Rico-Leo et al., 2016), embryonic stem cells (Ko et al., 2016; Wang et al., 2016), skin epithelia (Rico-Leo et al., 2013), melanoma (Contador-Troca et al., 2013; Contador-Troca et al., 2015), osteoblasts (Sharan et al., 2011; Yu et al., 2014) and embryonic teratocarcinoma cells (Morales-Hernandez et al., 2016).

The involvement of AhR in tissue regeneration has been analyzed in zebrafish exposed to the AhR carcinogenic ligand TCDD (2,3,7,8-tetrachlorodibenzo-p-dioxin). Following surgical amputation, TCDD inhibited caudal fin and heart regeneration at the larvae stage but not in adult zebrafish, suggesting that AhR activation by TCDD interferes with tissue repair at early stages of development in this non-mammalian animal model (Hofsteen et al., 2013; Mathew et al., 2006). Leflunomide, an anti-inflammatory drug and a proposed AhR agonist induced epimorphic re-growth of amputated zebrafish fin, further supporting the implication of AhR in tissue regeneration (O'Donnell et al., 2010). TCDD pre-treatment also reduced liver regeneration in mice after two-third partial hepatectomy, presumably by regulating cell cycle at the level of the cyclin-dependent kinase inhibitors $p21^{Cip1}$ and $p27^{Kip1}$ (Jackson et al., 2014; Mitchell et al., 2006).

In this study, we have exposed AhR wild type ($AhR^{+/+}$) and AhR-null ($AhR^{-/-}$) mice to naphthalene (NPH), a non-AhR-ligand toxic molecule, to investigate how AhR deficiency affects lung regeneration. The analyses of specific lung progenitor cell types and pluripotency markers revealed that $AhR^{-/-}$ mice have an increased efficiency to repair tissue damage, most probably because of an earlier and more efficient activation of stem-like cell subpopulations. These results agree with the current interest in the field to develop non-toxic AhR modulators potentially useful to improve tissue repair after toxic injury, surgical intervention or diseased states producing chronic lesions.

2. Materials and methods

2.1. $AhR^{+/+}$ and $AhR^{-/-}$ mice and treatments

$AhR^{+/+}$ and $AhR^{-/-}$ mice were generated by gene targeting as previously described (Fernandez-Salguero et al., 1995). Female mice were used in this study since previous reports have shown that whereas male mice develop tolerance for naphthalene, females trigger a much more sensitive response against this toxin (North et al., 2008; Sutherland et al., 2012). $AhR^{+/+}$ and $AhR^{-/-}$ females at 6 to 8 weeks of age were treated with a single i.p. dose of 250 mg/kg NPH (Sigma-Aldrich) dissolved in corn oil; control mice received the same volume of corn oil. Following treatment, mice were sacrificed at 2, 10 or 21 days and their lungs removed and processed for analysis. All work involving mice has been performed in accordance with the National and European legislation (Spanish Royal Decree RD53/2013 and EU Directive 86/609/CEE as modified by 2003/65/CE, respectively) for the protection of animals used for research. Experimental protocols using mice were approved by the Bioethics Committee for Animal Experimentation of the University of Extremadura (Registry 109/2014) and by the Junta de Extremadura (EXP-20160506-1). Mice had free access to water and rodent chow.

2.2. Antibodies and reagents

The following antibodies were used: anti-AhR (ENZO RPT 1:100 for lung, and Immunostep EB11767 1:50 for liver), anti E-cadherin (Invitrogen 13-1900, 1:100), anti-Ki67 (Santa Cruz Biotechnology sc-15,402, 1:200), anti-cytokeratin 14 (CK14) (COVANCE AF64 1:100), anti-CGRP (Santa Cruz Biotechnology sc-8856, 1:100), anti-CC10/Scgb1a1 (Origene TA322860 1:150), anti-OCT4 (Santa Cruz Biotechnology sc-5279, 1:200), anti-NANOG (Novus Biologicals NBP2-13177SS 1:50), anti-Shh (Novus Biologicals NBP2-22139SS 1:100).

2.3. Hematoxylin/eosin staining

Lung tissues were extracted and fixed overnight at room temperature in buffered formalin and included in paraffin. Sections were obtained at 4 μm, deparaffinated in xylol and gradually re-hydrated to distilled water. Sections were then incubated with hematoxylin for 3 min, washed with tap water and stained with eosin for 1 min. A final washing step was performed and tissues were de-hydrated, mounted and observed in a NIKON TE2000U microscope equipped with 4× (0.10 numeric aperture), 10× (0.25 numeric aperture) and 20× (0.40 numeric aperture) objectives.

2.4. Immunohistochemistry

Lung sections (3 μm) were obtained, deparaffinated and gradually re-hydrated to PBS. Sections were then incubated for 45 min in PBS containing 0.25% Triton X-100 (PBS-T) and 0.3% H_2O_2 to block endogenous peroxidase activity. After washing in PBS-T, unspecific binding was blocked by incubation in PBS-T containing 2 mg/ml gelatin (PBS-T-G) and 0.1 M lysine. The corresponding primary antibodies diluted in PBS-T-G were added for 16–18 h at the concentrations indicated above. Following washing in PBS-T-G, sections were incubated for 1 h at room temperature with the corresponding biotin-conjugated secondary antibody. After a final washing step in PBS-T-G, the streptavidin-peroxidase complex was added and the presence of target proteins revealed with diaminobenzidine (DAB). Nuclei were counterstained with Harris hematoxylin and sections de-hydrated and mounted using Eukitt (Kindler GmBH). A NIKON TE2000U microscope equipped with 4× (0.10 numeric aperture), 10× (0.25 numeric aperture) and 20× (0.40 numeric aperture) objectives was used for microscopic observation.

2.5. Immunofluorescence

Lung sections (3 μm) were initially processed as indicated above but omitting the blocking step with H_2O_2. Non-specific epitopes were blocked by incubation for 1 h at room temperature in PBS containing 0.05% Triton X-100 (TBS-T), 0.2% gelatin and 3% BSA. Sections were incubated overnight at 4 °C with the corresponding primary antibodies diluted in PBS-T containing 0.2% gelatin. Following washing in this same gelatin solution, sections were incubated for 1 h at room temperature with Alexa-488 or Alexa-633 labeled secondary antibodies. After additional washing, sections were dehydrated, mounted on Mowiol and visualized using an Olympus FV1000 confocal microscope (Olympus). Objectives used were: 10× (0.40 numeric aperture) and 20× (0.70 numeric aperture). Fluorescence analysis was done using the FV10 software (Olympus). DAPI was used to stain cell nuclei.

2.6. Cell sorting and pluripotent stem cell isolation

To quantify and to isolate pluripotent stem cells, lungs were extracted and processed essentially as described with some modifications (Gadepalli et al., 2013). In brief, lungs were initially perfused through the trachea with a Dispase solution (PBS containing 0.5 U/ml Dispase) to improve tissue digestion. Next, lungs were finely minced in PBS and rotated for 30 min at 37 °C in digestion solution (PBS containing 0.5 U/ml Dispase and 60 U/ml collagenase (Invitrogen)). Digested lungs were homogenized by pipetting and passing through a 21gauge syringe, filtered by a 0.40 μm mesh and centrifuged at 300 *g* for 5 min. Cell pellets were resuspended in sorting medium (PBS containing 10% FBS) prior to use. To quantify the number of pluripotent stem cells, samples were stained according to the $Sca1^+/CD31^-/CD45^-$ phenotype

and analyzed using a MoFlo Astrios EQ flow cytometer (Beckman Coulter). To isolate lung pluripotent stem cells for further analyses, cell pellets were processed by magnetic separation using the Pluripotent Stem Cell Isolation kit (Miltenyi Biotec) and the autoMACS Separator flow cytometer following the instructions provided by the manufacturer.

2.7. Reverse transcription and real-time PCR

Lungs were obtained at the different times and stored at −80 °C until use. Total lung RNA was purified by a two-step protocol. Firstly, tissues were grinded in liquid nitrogen, extracted in a Trizol reagent (Ambion)/chloroform solution, centrifuged and the aqueous supernatant precipitated with isopropanol and centrifuged at 15.000 *g* for 30 min at 4 °C. Secondly, dried pellets were dissolved in DEPC-treated water and the RNA-containing solutions further purified using the High Pure RNA Isolation Kit (Roche). Reverse transcription was performed using random priming and the iScript Reverse Transcription Super Mix (Bio-Rad). Real-time PCR (qPCR) was done using SYBR® Select Master Mix (Life Technologies) in a Step One Thermal Cycler (Applied Biosystems) essentially as described (Morales-Hernandez et al., 2016; Rico-Leo et al., 2016). *Gapdh* was used to normalize gene expression (ΔCt) and $2^{-\Delta\Delta Ct}$ to calculate changes in mRNA levels with respect to control or untreated conditions. The following primer sequences were used: *Oct4* 5′-CACGAGTGGAAAGCAACTCA-3′ (forward) and 5′-TTCATGTCCTGGGACTCCTC-3′ (reverse); *Nanog* 5′-AAGTACCTC AGCCTCCAGCA-3′ (forward) and 5′-GTGCTGAGCCCTTCTGAATC-3′ (reverse); *Shh* 5′-CTGGCCAGATGTTTTCTGGT-3′ (forward) and 5′-GATGTCGGGGTTGTAATTGG-3′ (reverse); *Gli1* 5′-CAGGAGTCCTTGCTCT GTCC-3′ (forward) and 5′-AGATTAAGAGGCCCCCAAGA-3′ (reverse); *Gapdh* 5′-TGAAGCAGGCATCTGAGGG-3′ (forward) and 5′-CGAAGG TGGAAGAGTGGGAG-3′ (reverse).

2.8. Statistical analyses

Quantitative data are shown as mean ± SD. Comparisons between experimental conditions was done using GraphPad Prism 6.0 software (GraphPad). The student's *t*-test was used to analyze differences between two experimental groups and ANOVA for the analyses of three or more groups. The Mann-Whitney non-parametric statistical method was used to compare rank variations between independent groups.

3. Results

3.1. AhR depletion accelerates lung regeneration after naphthalene-induced injury

Histological examination of the bronchiolar epithelium under basal conditions (untreated, UT) did not reveal significant overt differences between $AhR^{-/-}$ and $AhR^{+/+}$ mice (Fig. 1A,B). Two days after a single acute dose of naphthalene (NPH), a very similar destruction of the bronchiolar epithelium was observed in $AhR^{+/+}$ and $AhR^{-/-}$ female mice (Fig. 1A,B), indicating that AhR-null mice were equally sensitive than AhR wild type mice to this toxin. Interestingly, regeneration of the bronchiolar epithelium took place earlier in absence of AhR since by day 10

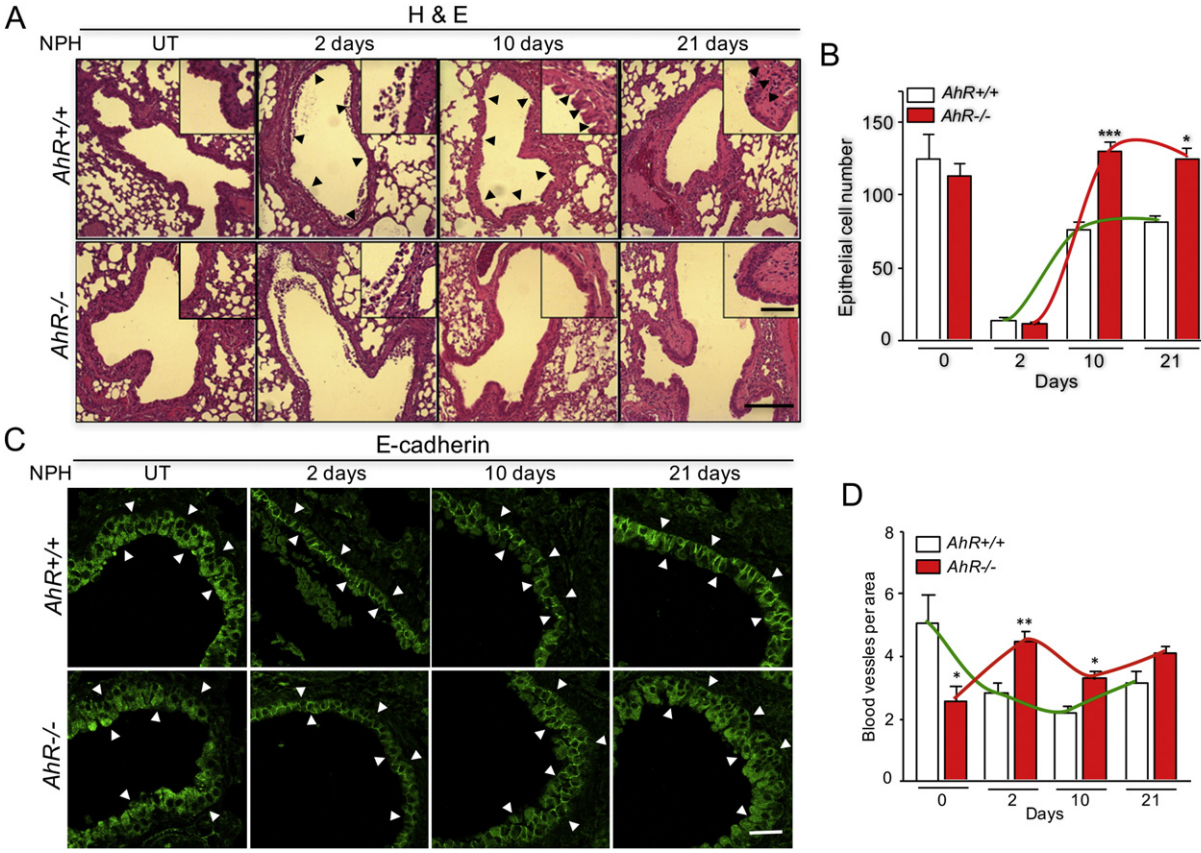

Fig. 1. AhR knock-out accelerates regeneration of the bronchiolar epithelium after naphthalene injury. $AhR^{+/+}$ and $AhR^{-/-}$ female mice were left untreated (UT) or treated with 250 mg/kg NPH and bronchiolar epithelium analyzed after 2, 10 and 21 days. (A) Hematoxylin-eosin (H&E) staining of lung sections. (B) Epithelial cells were counted for each mouse genotype and each time point. Data are shown as the number of epithelial cells per bronchiole a counted using a 10× objective in a NIKON TE2000U light microscope. (C) Immunofluorescence for the adherent junctions E-cadherin protein was used to further reveal the timing of regeneration in both genotypes. An Alexa 488-conjugated secondary antibody was used. (D) Changes in endothelium after NPH exposure were also determined by counting the number of blood vessels. Results are presented as the number of blood vessels counted per unit area using a 10× objective in a NIKON TE2000U light microscope. Details of the micrographs are shown in the insets. Two to three biological replicates and at least 5 experimental sections from each mouse were analyzed. A NIKON TE2000U microscope was used to visualize H & E staining. An Olympus FV1000 confocal microscope and the FV10 software (Olympus) were used for immunofluorescence. Data are shown as mean ± SD. *p < 0.05, **p < 0.01, ***p < 0.001. Bars: panel 1A: 100 μm, panel 1C: 25 μm, inset: 30 μm.

after treatment, $AhR^{-/-}$ mice already recovered their basal numbers of epithelial cells (Fig. 1A,B). $AhR^{+/+}$ mice showed a regenerative response that did not completely reconstruct the epithelium until 21 days from NPH exposure (Fig. 1A,B). To further support the more efficient tissue repair in AhR deficient mice, E-cadherin immunofluorescence was used to label the different epithelial cell layers of the bronchiolar epithelium. Indeed, despite a similar sensitivity to NPH (2 days), tissue repair proceeded faster in $AhR^{-/-}$ mice than in their counterparts $AhR^{+/+}$ mice (Fig. 1C). It has been suggested that the endothelium cross-talks with neighbour epithelial precursors to enhance their cell-autonomous regenerative potential (Ding et al., 2011; Yamamoto et al., 2007). Endothelial cell analysis showed that regardless a reduced content in basal blood vessels, AhR-null mice developed an earlier and more sustained vascular response to NPH than AhR wild type mice, whose vascularization remained suppressed even at latter times after treatment (Fig. 1D). The faster regenerative reaction observed in $AhR^{-/-}$ mice was confirmed by quantifying the number of proliferating Ki67 positive cells. Basal proliferation rates were very low in both $AhR^{+/+}$ and $AhR^{-/-}$ mice in bronchiolar and peribronchiolar epithelia (Fig. 2A). In the bronchiolar epithelium, the number of Ki67 + cells rapidly increased in $AhR^{-/-}$ mice 2 days after NPH exposure to decline to basal levels by 21 days (Fig. 2B, left panel); in $AhR^{+/+}$ mice, bronchiolar proliferation was delayed reaching its maximum at 10 days and remaining at high levels until 21 days (Fig. 2B, left panel). The profile of Ki67 expression in peribronchiolar cells again revealed an earlier response in $AhR^{-/-}$ than in $AhR^{+/+}$ mice, although proliferation continued elevated above basal levels in both genotypes even at 21 days after treatment (Fig. 2B, right panel).

3.2. Lack of AhR expands undifferentiated cell types in the regenerating bronchiolar epithelium

Several cell types can become activated to reconstitute the bronchoalveolar epithelium after severe NPH-induced injury. Most regeneration is produced by differentiation of NPH-resistant Clara cells lining the basal epithelium, although additional types including isolectin GSI-B4 reactive-cytokeratin 14 expressing cells and neuroepithelial precursors can be also involved (Giangreco et al., 2009; Giangreco et al., 2002; Rawlins et al., 2009; Reynolds et al., 2000; Song et al., 2012). We first decided to determine if AhR knock-out affected the global content in undifferentiated $Sca1^{+}/CD31^{-}/CD45^{-}$ cells considered representative of multipotent bronchiolar stem cells (Gadepalli et al., 2013; Gong et al., 2014; Teisanu et al., 2009). Flow cytometry analysis for $Sca1^{+}/CD31^{-}/CD45^{-}$ indicated that $AhR^{-/-}$ lungs had an increased amount of multipotent stem cells under basal physiological conditions (Fig. 3A). Based on this observation, we then examined the profile of

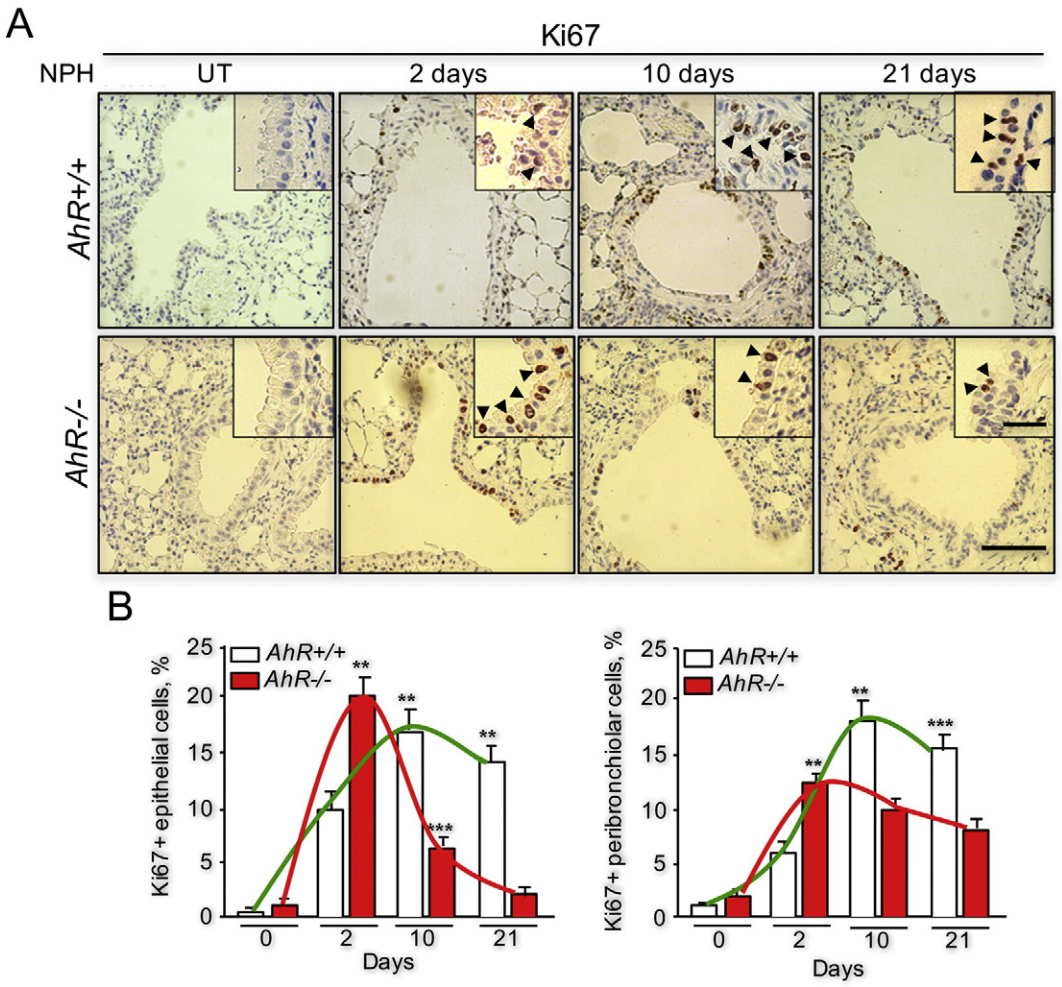

Fig. 2. Lack of AhR triggers a faster proliferative response in the bronchiolar and peribronchiolar epithelia. $AhR^{+/+}$ and $AhR^{-/-}$ female mice were left untreated (UT) or treated with 250 mg/kg NPH and bronchiolar epithelium analyzed after 2, 10 and 21 days. (A) Proliferation was analyzed by immunohistochemistry in lung sections using Ki67 as a marker. (B) The number of Ki67 + cells was counted in the bronchiolar (left panel) and peribronchiolar (right panel) regions of the lungs at the different time points analyzed. Data are represented as the number of Ki67 + cells per the total number of epithelial cells per bronchiole (left panel) or the number of Ki67 + cells per unit area using a 10× objective in a NIKON TE2000U light microscope. At least 500 cells were counted per biological replicate. Details of the micrographs are shown in the insets. Two to three biological replicates and at least 5 experimental sections from each mouse were analyzed. A NIKON TE2000U microscope was used for immunohistochemistry. Data are shown as mean ± SD. $^{**}p < 0.01$, $^{***}p < 0.001$. Bar: 100 μm, inset: 25 μm.

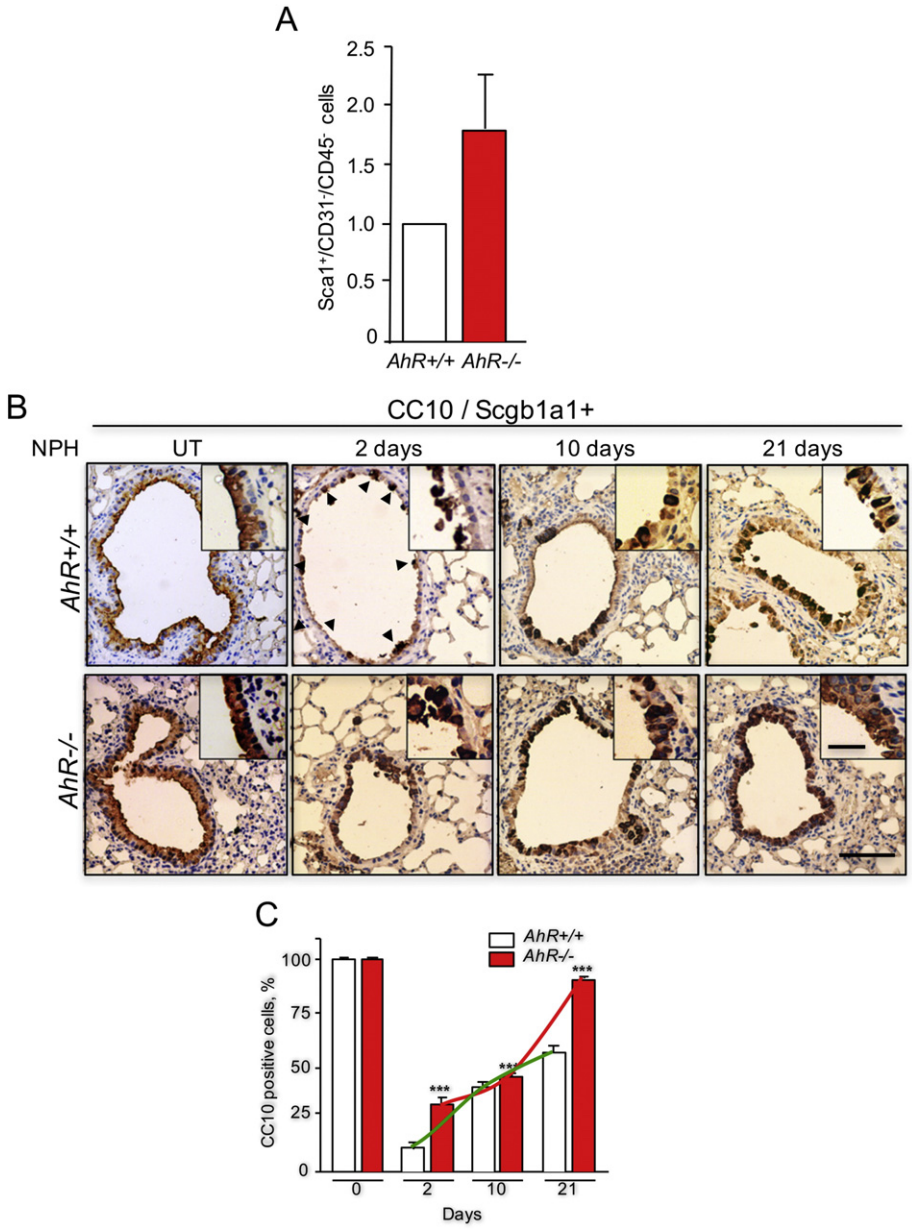

Fig. 3. AhR modulates stem-like and Clara cells in the lung. $AhR^{+/+}$ and $AhR^{-/-}$ female mice were left untreated (UT) or treated with 250 mg/kg NPH and bronchiolar epithelium analyzed after 2, 10 and 21 days. (A) Lungs were extracted and processed to obtain cell suspensions that were stained for the $Sca1^{+}/CD31^{-}/CD45^{-}$ profile. Cells were analyzed using a MoFlo Astrios EQ flow cytometer (Beckman-Coulter). The number of $Sca1^{+}/CD31^{-}/CD45^{-}$ cells was referred to the total number of cells counted by the flow cytometer for each genotype. The percentage of $Sca1^{+}/CD31^{-}/CD45^{-}$ cells in $AhR^{-/-}$ lungs has been compared to that in $AhR^{+/+}$ lungs (set to 1). (B) Lung sections were prepared and immunostained for Clara cells using the CC10/Scgb1a1 marker. (C) The number of bronchiolar positive cells were counted and plotted for the different experimental times. Details of the micrographs are shown in the insets. Two to three biological replicates and at least 5 experimental sections from each mouse were analyzed. A NIKON TE2000U microscope was used for immunohistochemistry. Data are shown as mean ± SD. ***$p < 0.001$. Bar: 100 μm, inset: 25 μm.

undifferentiated precursor cell lineages in NPH-exposed $AhR^{+/+}$ and $AhR^{-/-}$ bronchiolar epithelium. Immunohistochemical analysis using the Clara cell-specific marker CC10/Scgb1a1 (Secretoglobin 1a1) (Volckaert and De Langhe, 2014) showed that AhR deficiency did not alter endogenous Clara cell numbers and that NPH was very efficient in depleting this cell type in the bronchiolar epithelium (Fig. 3B). CC10/Scgb1a1 positive cells rapidly and steadily increased in $AhR^{-/-}$ lungs from 2 days after NPH treatment until the end of the regenerative process; CC10/Scgb1a1 positive cells also expanded in $AhR^{+/+}$ lungs, although with a slower and less pronounced kinetic that did not reach basal values by 21 days (Fig. 3B).

Isolectin GSI-B4 reactive cells, expressing the undifferentiation marker cytokeratin 14 (CK14), can differentiate to Clara cells upon NPH exposure. We have used immunofluorescence for CK14 to determine the contribution of this cell type to the regenerative process. In absence of significant differences under basal tissue conditions, $AhR^{-/-}$ mice produced an earlier and transient increase in CK14+ cells reaching highest values at 2 days to decrease to initial levels by 21 days (Fig. 4A). $AhR^{+/+}$ mice, on the contrary, did not significantly expanded CK14+ cells in response to NPH and showed a moderate decrease at later stages (e.g. 21 days) of regeneration (Fig. 4A). Interestingly, $AhR^{-/-}$ mice had similar profiles of CK14 and Ki67 positivity in the regenerating bronchiolar epithelium.

Neuroepithelial precursors can differentiate to Clara cells after NPH-induced injury (Volckaert and De Langhe, 2014). We then performed immunofluorescence for the calcitonin-gene related peptide (CGRP) that is considered specific for pulmonary neuroendocrine cells (Song et al., 2012). $AhR^{-/-}$ mice had significantly increased basal amounts of

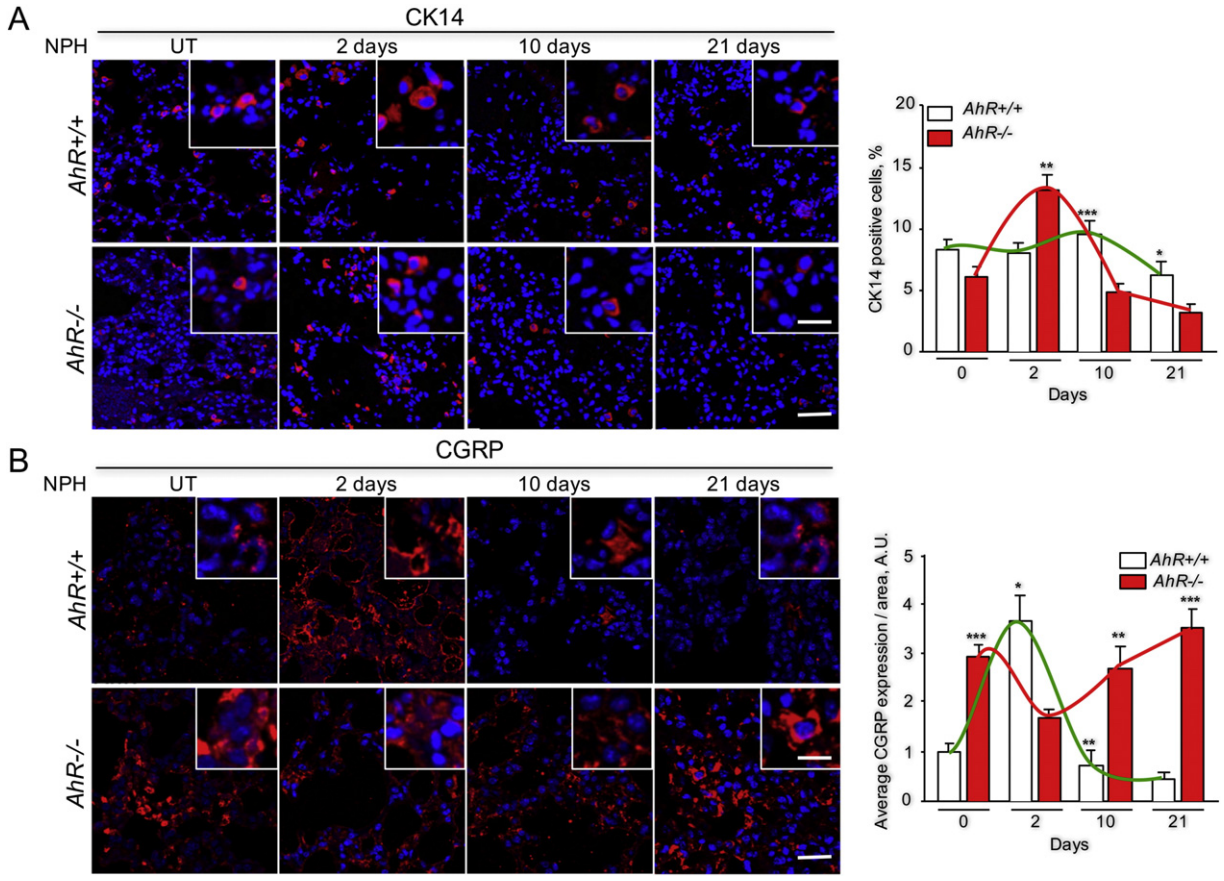

Fig. 4. Levels of bronchiolar precursors generating Clara cells are enhanced in $AhR^{-/-}$ lungs. $AhR^{+/+}$ and $AhR^{-/-}$ female mice were left untreated (UT) or treated with 250 mg/kg NPH and bronchiolar epithelium analyzed after 2, 10 and 21 days. (A) Generation of isolectin GSI-B4 reactive cells expressing the undifferentiation marker CK14 were quantified by immunofluorescence using an anti-CK14 specific antibody. (B) Neuroepithelial precursors were analyzed by immunofluorescence using the calcitonin-gene related peptide (CGRP) as marker. Details of the micrographs are shown in the insets. Two to three biological replicates and at least 5 experimental sections from each mouse were analyzed. An Alexa 633-conjugated secondary antibody was used for detection. DAPI staining was used to label cell nuclei. An Olympus FV1000 confocal microscope and the FV10 software (Olympus) were used for immunofluorescence. Data are shown as mean ± SD. *$p < 0.05$, **$p < 0.01$, ***$p < 0.001$. Bars: 50 μm, inset: 25 μm.

CGRP + cells with respect to $AhR^{+/+}$ mice (Fig. 4B). Following NPH treatment, the number of neuroepithelial cells transiently decreased at 2 days in $AhR^{-/-}$ lungs to fully recover to pre-treatment values at 21 days. $AhR^{+/+}$ mice developed an inverse response increasing CGRP + cells at shorter times to decrease to initial values at the end of regeneration (Fig. 4B). Intriguingly, the transient decrease in neuroepithelial cells observed shortly after injury in $AhR^{-/-}$ lungs appeared synchronized with the transient increase in CK14 + and Clara cells and with their enhanced proliferation rates.

3.3. Pluripotency markers are modulated in an AhR-dependent manner during lung regeneration

We, and others, have shown that AhR is involved in the regulation of pluripotency-inducing genes such as OCT4/POU5F1 (Bunaciu and Yen, 2011; Cheng et al., 2015; Morales-Hernandez et al., 2016), NANOG (Morales-Hernandez et al., 2016) and SOX2 (Contador-Troca et al., 2015). We therefore decided to investigate if the accelerated regeneration observed in $AhR^{-/-}$ mice could be associated to a differential expression in AhR-related pluripotency markers. Immunofluorescence analysis revealed a significant upregulation of OCT4/POU5F1 in basal $AhR^{-/-}$ bronchiolar epithelium as compared to $AhR^{+/+}$ lung (Fig. 5A). NPH treatment induced a slight decrease in OCT4/POU5F1 levels from 2 to 10 days in $AhR^{-/-}$ mice that regained initial values by 21 days. $AhR +/+$ lungs treated with NPH transiently increased bronchiolar OCT4/POU5F1 expression at 2 days to then return to pre-treatment levels at 21 days (Fig. 5A). In $AhR^{-/-}$ lungs, NANOG was also upregulated under basal tissue conditions and its expression markedly decayed at 10 days to partially recover at 21 days after NPH exposure (Fig. 5B). NANOG was rapidly downregulated by NPH in $AhR^{+/+}$ bronchiolar epithelium decreasing at 2 days after treatment to moderately increase from 10 to 21 days (Fig. 5B). Thus, constitutive upregulation of OCT4/POU5F1 and NANOG could give $AhR^{-/-}$ lungs an advantage to respond against NPH injury. To analyze if OCT4/POU5F1 and NANOG overexpression could be related to the presence of undifferentiated cells in the basal epithelium, flow cytometry was used to isolate stem-like cells from naive $AhR^{+/+}$ and $AhR^{-/-}$ lungs. Quantitative mRNA analyses for *Oct4* and *Nanog* in isolated stem-like cells revealed that both genes were significantly upregulated in untreated $AhR^{-/-}$ lungs (Fig. 6A), further supporting that AhR deficiency contributes to the generation of a primed status favoring an early repair response. We then decided to determine *Oct4* and *Nanog* mRNA levels in NPH-treated lungs. Interestingly, the profile of *Oct4* mRNA expression before and after NPH treatment (Fig. 6B) closely followed that of OCT4 protein as determined by immunofluorescence (see Fig. 5A). *Nanog* mRNA expression had a qualitatively similar pattern to that of NANOG protein (see Fig. 5B), although no significant differences were observed in mRNA between $AhR^{+/+}$ and $AhR^{-/-}$ lungs (Fig. 6C).

Recent studies have shown that the ligand of the Hedgehog (Hh) pathway Sonic Hedgehog (Shh) is expressed in Scgb1a1 + cells of the proximal adult lung epithelium, and that Hh signaling becomes downmodulated at the acute phase of lung injury to regain normal levels during regeneration (Peng et al., 2015). Since absence of AhR influenced the appearance of CC10/Scgb1a1 + cells during tissue repair in

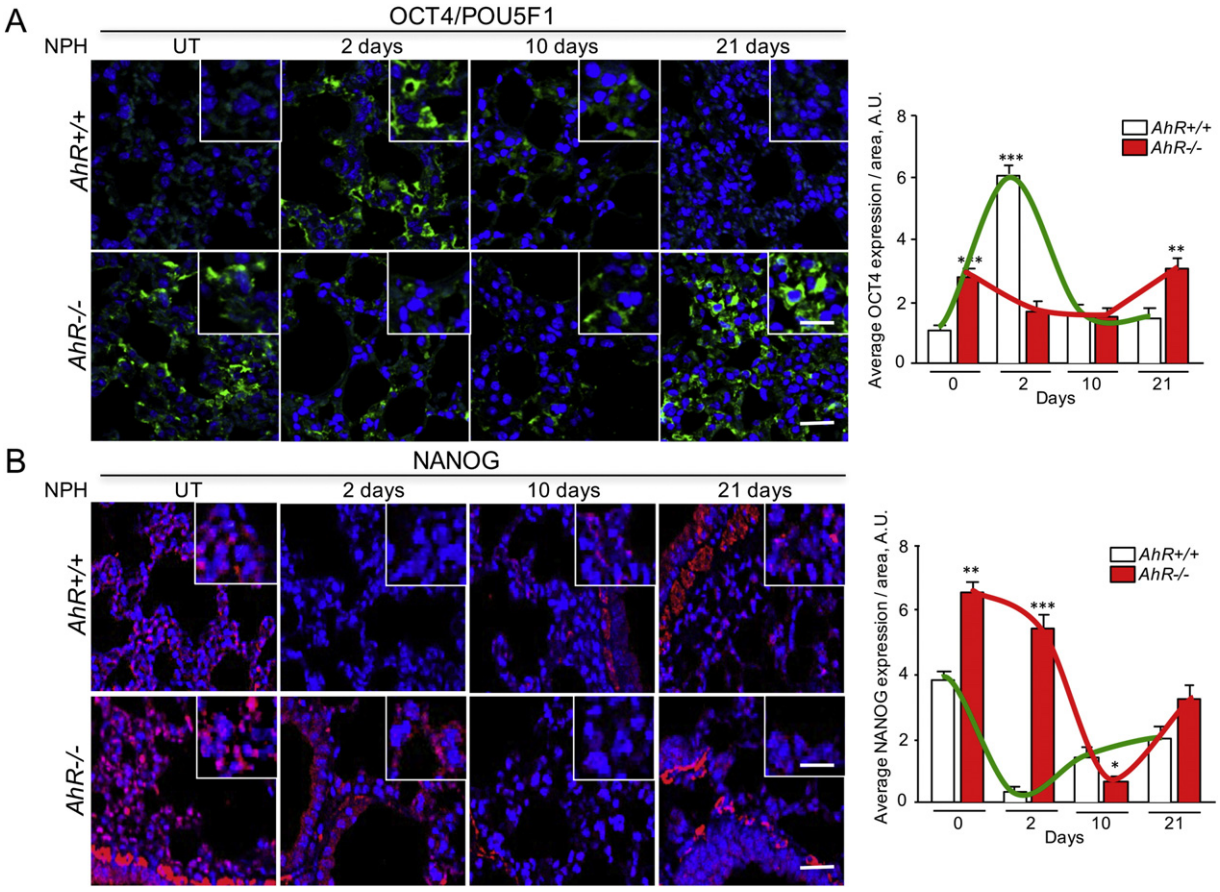

Fig. 5. Pluripotency-related factors OCT4/POU5F1 and NANOG are differentially regulated during regeneration of the bronchiolar epithelium. $AhR^{+/+}$ and $AhR^{-/-}$ female mice were left untreated (UT) or treated with 250 mg/kg NPH and bronchiolar epithelium analyzed after 2, 10 and 21 days. (A) OCT/POU5F1 was analyzed by immunofluorescence in lung sections of each mouse genotype using a specific antibody. An Alexa 488-conjugated secondary antibody was used for detection. (B) NANOG levels were determined by immunofluorescence in the same lung sections indicated above. Details of the micrographs are shown in the insets. An Alexa 633-conjugated secondary antibody was used for detection. DAPI staining was used to label cell nuclei. Two to three biological replicates and at least 5 experimental sections from each mouse were analyzed. An Olympus FV1000 confocal microscope and the FV10 software (Olympus) were used for immunofluorescence. Data are shown as mean ± SD. $^{**}p < 0.05$, $^{**}p < 0.01$, $^{***}p < 0.001$. Bars: 50 μm, inset: 25 μm.

NPH treated mice, we decided to use immunofluorescence to examine Shh expression in the bronchiolar epithelium of $AhR^{+/+}$ and $AhR^{-/-}$ mice. In agreement with previous reports, Shh was transiently downregulated in $AhR^{+/+}$ lungs at the beginning of the regeneration process (e.g. 2 days) returning to its basal levels by 10 and 21 days (Fig. 7A). $AhR^{-/-}$ lungs had reduced basal expression of Shh protein that gradually increased from 2 to 10 days after treatment to return to basal levels at 21 days (Fig. 7A). mRNA analysis revealed that $AhR^{-/-}$ lungs had reduced basal levels of *Shh* that were not repressed at 2 days after NPH treatment and that transiently increased from 10 to 21 days (Fig. 7B). $AhR^{+/+}$ lungs expressed higher basal amounts of *Shh* mRNA that remained slightly reduced from 2 to 21 days from treatment (Fig. 7B). The fact that complete downregulation of Shh did not seem required to trigger regeneration in $AhR^{-/-}$ mice was intriguing. We considered the possibility that the subpopulation of stem-like cells present in $AhR^{-/-}$ mice under basal conditions could have reduced expression of inhibitory *Shh*. mRNA analysis of flow cytometry isolated stem-like cells revealed a significant repression of *Shh* in $AhR^{-/-}$ lungs as compared to $AhR^{+/+}$ lungs (Fig. 7C). The effector of the Hedgehog pathway Glioma-associated oncogene homolog-1 (*Gli1*) was also significantly repressed in $AhR^{-/-}$ stem-like cells (Fig. 7D), suggesting that downmodulation of inhibitory Shh signaling in $AhR^{-/-}$ undifferentiated precursors might contribute to improve regeneration.

Based on the different regenerative potential existing between $AhR^{+/+}$ and $AhR^{-/-}$ mice, we decided to determine whether AhR itself was regulated during lung repair. Immunofluorescence analysis showed that basal AhR expression was severely repressed in $AhR^{+/+}$ lungs between 2 and 10 days to return to its initial levels by 21 days (Fig. 7E). As expected, $AhR^{-/-}$ bronchiolar epithelium completely lacked AhR expression (Fig. 7E). Thus, AhR may need to be downregulated early after NPH-induced damage to facilitate lung regeneration.

4. Discussion

Certain mammalian tissues, such as lung and liver, have the ability to regenerate after exposure to environmental toxicants, as a consequence of accidental damage or following surgical intervention. One aspect currently under close scrutiny is to discover the identity of the precursor cell lineages that trigger the regenerative response. In the lung, the activation and differentiation of pluripotent/multipotent stem-like cells appear relevant for repair following interaction with damaging toxins (Kotton and Morrisey, 2014; Leeman et al., 2014). Also relevant is to characterize the molecular intermediates controlling the differentiation of stem-like cells that will produce the cell types required to restore tissue structure and function.

AhR is one such potential molecular intermediate since it is involved in maintaining differentiation of normal and transformed cells (reviewed in (Mulero-Navarro and Fernandez-Salguero, 2016)) and in regulating pluripotency-related genes OCT4, NANOG and SOX2 (Bunaciu and Yen, 2011; Cheng et al., 2015; Contador-Troca et al., 2015; Morales-Hernandez et al., 2016). In a non-mammalian context, AhR inhibits caudal fin and heart regeneration in zebrafish upon TCDD

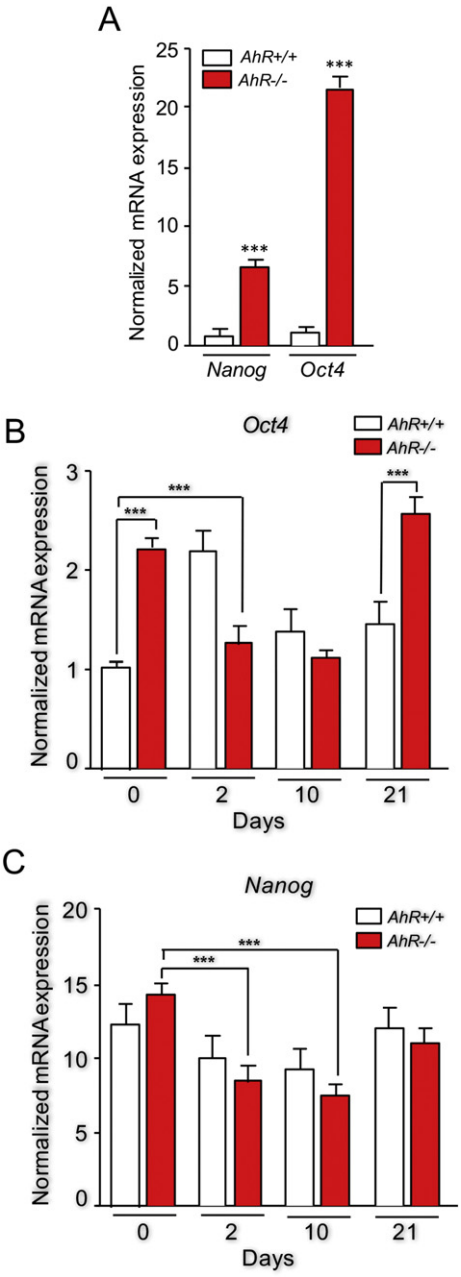

Fig. 6. *Oct4* and *Nanog* mRNA expression in lung stem-like cells and NPH-treated lungs. (A) Lungs from untreated $AhR^{+/+}$ and $AhR^{-/-}$ female mice were processed to isolate stem-like cells using magnetic-assisted flow cytometry. mRNA levels of *Oct4* and *Nanog* were analyzed by RT-qPCR in those pluripotent cells from each genotype. (B and C) $AhR^{+/+}$ and $AhR^{-/-}$ female mice were left untreated (UT) or treated with 250 mg/kg NPH and their lungs extracted at 2, 10 and 21 days. *Oct4* (B) and *Nanog* (C) mRNA expression was analyzed at each time point by RT-qPCR using total lung RNA. Oligonucleotides for each gene are indicated in the Methods. Gene expression has been normalized by *Gapdh* and represented as $2^{-\Delta\Delta Ct}$. Two to three biological replicates and at least 4 experimental replicates from each mouse were analyzed. Data are shown as mean ± SD. ***$p < 0.001$.

exposure (Hofsteen et al., 2013; Mathew et al., 2006) whereas, in mammals, TCDD treatment prior to two third partial hepatectomy suppressed mouse liver regeneration by blocking cell cycle through inhibition of cyclin-dependent kinase-2 (CDK2) (Jackson et al., 2014; Mitchell et al., 2006). To the best of our knowledge, there are no previous studies addressing the implication of AhR in lung regeneration. Here, we have used AhR-null mice to investigate if endogenous AhR expression affects lung regeneration in response to injury caused by the non-AhR-ligand toxic molecule naphthalene. The major conclusion of the study is that absence of AhR increases the efficiency and expedites lung regeneration likely by activating the differentiation of stem-like precursors and by modulating the expression of pluripotency-inducing factors.

Naive AhR-null mice had similar numbers of bronchiolar epithelial cells and were equally sensitive than wild type mice to NPH-induced lung injury, thus excluding the existence of developmental alterations that could influence their regenerative potential. Increased regeneration of $AhR^{-/-}$ lungs likely depended on an early proliferative response in the otherwise non-proliferating lung epithelium, in agreement with the well-known role of AhR in controlling cell proliferation and cell cycle (Barouki et al., 2007; Marlowe et al., 2004; Marlowe and Puga, 2005; Pohjanvirta, 2012; Puga et al., 2002). Cell proliferation after NPH exposure is closely linked to a differentiation program of precursor cells residing in the bronchioalveolar epithelium (Volckaert and De Langhe, 2014). Clara cells are considered the predominant cell type responsible for restoring the bronchiolar epithelium after NPH toxicity (Giangreco et al., 2009; Giangreco et al., 2002; Reynolds et al., 2000). In agreement with these previous reports, Clara cells were steadily produced at a higher level in $AhR^{-/-}$ than in $AhR^{+/+}$ NPH-exposed lungs. Since basal numbers of Clara cells did not significantly differ between both genotypes, our results suggest that their accumulation in AhR-null bronchiolar epithelium could derive from an increase in their auto-renewing capacity and/or their expansion from undifferentiated precursors.

Regarding the first possibility, it is known that Clara cells (Scgb1a1 + cells) can auto-renew and differentiate to ciliated cells in order to replenish a damaged bronchiolar epithelium (Kim et al., 2005; Rawlins et al., 2009). One potential regulator of Clara cell differentiation is the Hedgehog (Hh) signaling pathway that needs to be inhibited at early phases of NPH-induced toxicity to allow lung regeneration (Peng et al., 2015). Interestingly, we have found that AhR deficiency significantly inhibits constitutive expression of Hh ligand Shh and of Hh target *Gli1* in isolated lung stem-like cells, suggesting that lower inhibitory Hh signaling could favor their differentiation to regenerating Clara cells. To address the expansion of Clara cells from undifferentiated precursors, we analyzed the profiles of isolectin GSI-B4 reactive cells expressing CK14 and of CGRP + neuroepithelial cells. CK14 positive cells rapidly increased in $AhR^{-/-}$ lungs in response to NPH toxicity and such increase preceded the expansion of Clara cells. Because CK14 + cells can differentiate into several multipotent cell types (Clara cells among them) (Hong et al., 2004a,b), it is plausible that AhR deficiency increases the ability of the bronchiolar epithelium to activate stem-like CK14 + cells eventually generating Clara cells. Neuroepithelial cells expressing the calcitonin-gene related peptide (CGRP) (Song et al., 2012) do not differentiate to Clara cells under physiological conditions, but become activated after NPH injury (Volckaert and De Langhe, 2014). The bronchiolar epithelium of $AhR^{-/-}$ mice had significantly higher amounts of CGRP + cells than $AhR^{-/-}$ mice. Interestingly, this cell type decreased shortly after injury in $AhR^{-/-}$ mice concurrently with the raise in Clara cells, perhaps indicating that a fraction of basal CGRP + cells were differentiated into Clara cells. By contrast, CGRP + cells transiently increased in $AhR^{+/+}$ lungs soon after NPH treatment and prior to Clara cell accumulation. These results suggest that lack of AhR improved the initial stages of bronchiolar regeneration by increasing the production of Clara cells probably from upregulated CK14 + and neuroepithelial cell lineages. In addition to these cell-autonomous effects, $AhR^{-/-}$ lungs developed a greater vascular response shortly after NPH toxicity, despite a reduced basal content of blood vessels. AhR is required for vascularization and angiogenesis and for the development of the cardiovascular system (Lahvis et al., 2000; Lahvis et al., 2005; Roman et al., 2009; Sauzeau et al., 2011). It is therefore possible that AhR deficiency in the stroma could trigger angiogenesis to favor repair of the bronchiolar epithelium. Further studies are needed to determine whether those microenvironment-dependent effects involve cytokeratins regulated by AhR such as transforming

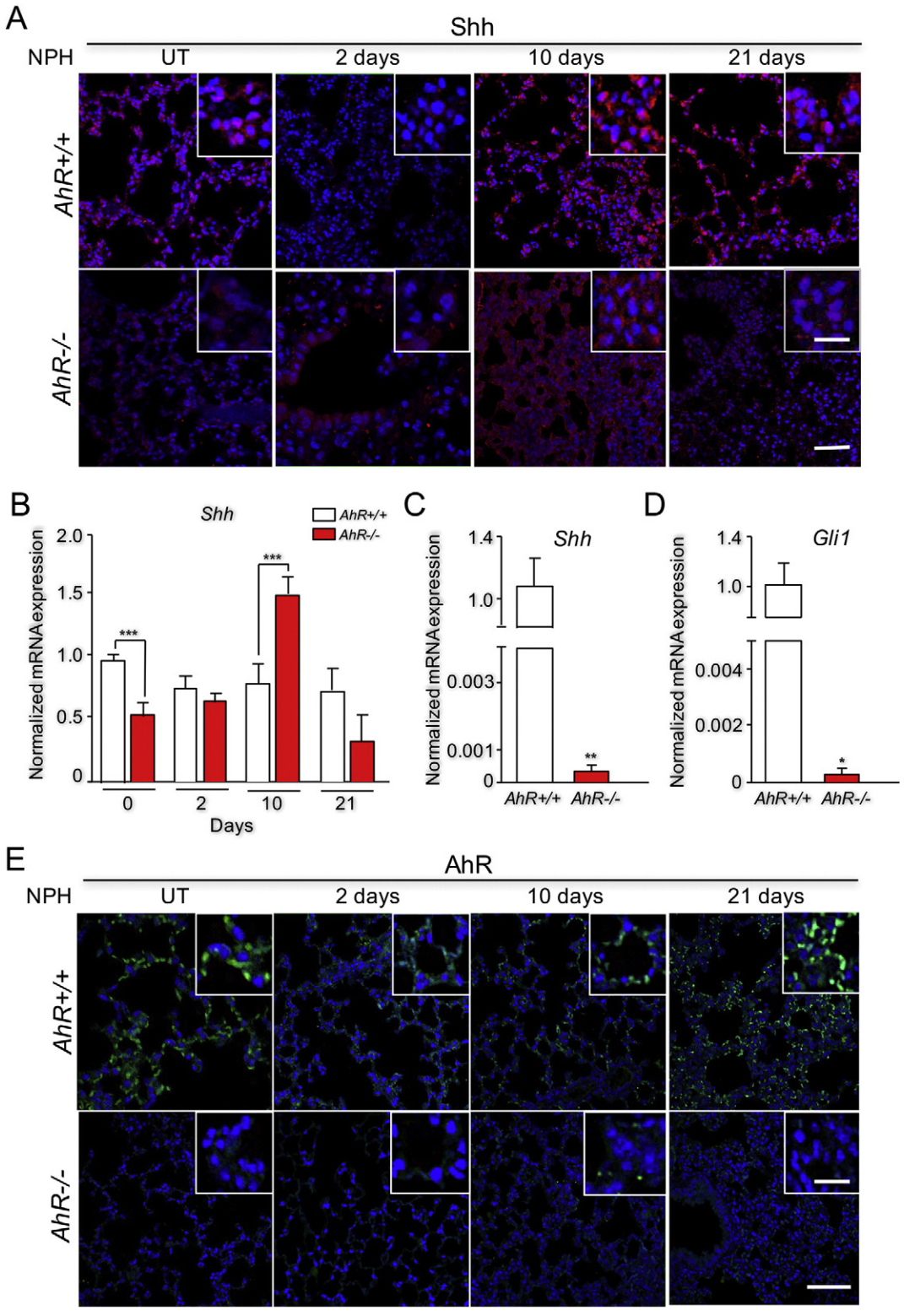

Fig. 7. Sonic-Hedgehog (Shh) and AhR are downregulated during lung regeneration in $AhR^{+/+}$ mice. $AhR^{+/+}$ and $AhR^{-/-}$ female mice were left untreated (UT) or treated with 250 mg/kg NPH and bronchiolar epithelium analyzed after 2, 10 and 21 days. (A) Shh expression was determined in lung sections by immunofluorescence using a specific antibody. An Alexa 633-conjugated secondary antibody was used. (B) *Shh* mRNA expression was analyzed at each time point by RT-qPCR using total RNA. (C and D) Lungs from basal $AhR^{+/+}$ and $AhR^{-/-}$ female mice were extracted and processed to isolate stem-like cells using magnetic-assisted flow cytometry. mRNA levels of *Shh* (C) and *Gli1* (D) were analyzed by RT-qPCR using total RNA obtained from stem-like cells of each genotype. Oligonucleotides used are indicated in the Methods. Gene expression has been normalized by *Gapdh* and represented as $2^{-\Delta\Delta Ct}$. (E) AhR levels were analyzed using a specific antibody in lung sections at the times indicated. Details of the micrographs are shown in the insets. An Alexa 488-conjugated secondary antibody was used for detection. DAPI staining was used to label cell nuclei. Two to three biological replicates and 4–5 experimental replicated from each mouse were analyzed. An Olympus FV1000 confocal microscope and the FV10 software (Olympus) were used for immunofluorescence. Bars: 50 μm, inset: 25 μm.

growth factor-β1 (TGFβ1) (Gomez-Duran et al., 2009; Rico-Leo et al., 2013).

AhR-dependent effects on lung regeneration also involve changes in pluripotency-related markers OCT4 and NANOG, both previously known to be regulated by this receptor in different cell types (Bunaciu and Yen, 2011; Cheng et al., 2015; Morales-Hernandez et al., 2016; Mulero-Navarro and Fernandez-Salguero, 2016). The upregulation of OCT4 and NANOG under basal conditions in $AhR^{-/-}$ mice could reflect the existence of an undifferentiated bronchiolar epithelium primed to develop a more efficient differentiation response during tissue repair. The upregulation of *Oct4* mRNA in $AhR^{-/-}$ lungs under basal conditions could not only determine its increased protein expression but also indicate that AhR controls *Oct4* at the transcriptional level in bronchiolar epithelial cells similarly to that reported in stem-like undifferentiated human carcinoma cells (Cheng et al., 2015; Morales-Hernandez et al., 2016). In agreement with OCT4 being a regeneration inducing factor in the lung, our data also showed that OCT4 expression increased in a synchronized manner with cell proliferation in $AhR^{+/+}$ bronchiolar epithelium at earlier times than the onset of tissue repair. NANOG protein was also overexpressed in basal $AhR^{-/-}$ lungs although no significant differences were found at the mRNA level, despite been also an AhR transcriptional target in stem-like human carcinoma cells (Morales-Hernandez et al., 2016). Interestingly, OCT4 and NANOG were downmodulated once regeneration started in both $AhR^{+/+}$ and $AhR^{-/-}$ lungs, suggesting that their expression was more relevant at the beginning of the process, perhaps resembling their effects in adult cell reprogramming (Nakagawa and Yamanaka, 2010; Takahashi and Yamanaka, 2016). In fact, the overexpression of *Oct4* and *Nanog* in isolated stem-like $AhR^{-/-}$ cells in absence of NPH may link the expression of these genes to the faster enrichment of Clara, Basal and neuroepithelial cells in AhR-null lungs. The lower expression of NANOG at early times (e.g. 2 days) in $AhR^{+/+}$ mice is intriguing although it could result from OCT4-dependent inhibition as previously reported (Pan et al., 2006).

5. Conclusions

In summary, physiological AhR deficiency improves the regenerative potential of the lung in response to the deleterious effects of acute toxin exposure. Such effects involve enhanced proliferation, a more efficient differentiation of cell lineages with stem-like properties and the upregulation of relevant pluripotency-related genes. AhR can be therefore a novel regulator of lung regeneration and tissue repair, a function potentially relevant considering the many toxic compounds interacting with the lung epithelium to induce pathologies such as emphysema, cancer and fibrosis. The characterization of AhR non-toxic antagonists could help identify molecules useful for tissue repair after exposure to environmental toxins and carcinogens. In this context, application of AhR modulators able to transiently reduce receptor functions at early stages of lung regeneration may be hypothetically consider novel tools with therapeutic value. Further investigations using conditional mouse models in which AhR can be knockdown within a defined time window may be useful to answer that question.

Acknowledgments

This work was supported by grants to P.M.F-S. from the Spanish Ministry of Economy and Competitiveness (SAF2014-51813-R) and from the Junta de Extremadura (GR15008 and IB16210). Research at P.M.F-S. laboratory was also funded by the Red Temática de Investigación Cooperativa en Cáncer (RTICC), Carlos III Institute, Spanish Ministry of Economy and Competitiveness (RD12/0036/0032). A.M.-H. was supported by the Junta de Extremadura and N.M.-M. and A.N.-P. by the Ministerio de Economía y Competitividad. B.P. was supported by Junta de Extremadura. All Spanish funding is co-sponsored by the European Union FEDER program.

The support and help of the Servicio de Técnicas Aplicadas a las Biociencias (STAB) of the Universidad de Extremadura is greatly acknowledged.

Conflicts of interest

The authors declare no conflicts of interest regarding this manuscript.

References

Barouki, R., Coumoul, X., Fernandez-Salgueroc, P.M., 2007. The aryl hydrocarbon receptor, more than a xenobiotic-interacting protein. FEBS Lett. 581, 3608–3615.

Bunaciu, R.P., Yen, A., 2011. Activation of the aryl hydrocarbon receptor AhR promotes retinoic acid-induced differentiation of myeloblastic leukemia cells by restricting expression of the stem cell transcription factor Oct4. Cancer Res. 71, 2371–2380.

Cheng, J., Li, W., Kang, B., Zhou, Y., Song, J., Dan, S., Yang, Y., Zhang, X., Li, J., Yin, S., Cao, H., Yao, H., Zhu, C., Yi, W., Zhao, Q., Xu, X., Zheng, M., Zheng, S., Li, L., Shen, B., Wang, Y.J., 2015. Tryptophan derivatives regulate the transcription of Oct4 in stem-like cancer cells. Nat. Commun. 6, 7209.

Contador-Troca, M., Alvarez-Barrientos, A., Barrasa, E., Rico-Leo, E.M., Catalina-Fernandez, I., Menacho-Marquez, M., Bustelo, X.R., Garcia-Borron, J.C., Gomez-Duran, A., Saenz-Santamaria, J., Fernandez-Salguero, P.M., 2013. The dioxin receptor has tumor suppressor activity in melanoma growth and metastasis. Carcinogenesis 34, 2683–2693.

Contador-Troca, M., Alvarez-Barrientos, A., Merino, J.M., Morales-Hernandez, A., Rodriguez, M.I., Rey-Barroso, J., Barrasa, E., Cerezo-Guisado, M.I., Catalina-Fernandez, I., Saenz-Santamaria, J., Oliver, F.J., Fernandez-Salguero, P.M., 2015. Dioxin receptor regulates aldehyde dehydrogenase to block melanoma tumorigenesis and metastasis. Mol. Cancer 14, 148.

Ding, B.S., Nolan, D.J., Guo, P., Babazadeh, A.O., Cao, Z., Rosenwaks, Z., Crystal, R.G., Simons, M., Sato, T.N., Worgall, S., Shido, K., Rabbany, S.Y., Rafii, S., 2011. Endothelial-derived angiocrine signals induce and sustain regenerative lung alveolarization. Cell 147, 539–553.

Eisenhauer, P., Earle, B., Loi, R., Sueblinvong, V., Goodwin, M., Allen, G.B., Lundblad, L., Mazan, M.R., Hoffman, A.M., Weiss, D.J., 2013. Endogenous distal airway progenitor cells, lung mechanics, and disproportionate lobar growth following long-term postpneumonectomy in mice. Stem Cells 31, 1330–1339.

Esser, C., Rannug, A., 2015. The aryl hydrocarbon receptor in barrier organ physiology, immunology, and toxicology. Pharmacol. Rev. 67, 259–279.

Esser, C., Rannug, A., Stockinger, B., 2009. The aryl hydrocarbon receptor in immunity. Trends Immunol. 30, 447–454.

Fernandez-Salguero, P., Pineau, T., Hilbert, D.M., McPhail, T., Lee, S.S., Kimura, S., Nebert, D.W., Rudikoff, S., Ward, J.M., Gonzalez, F.J., 1995. Immune system impairment and hepatic fibrosis in mice lacking the dioxin-binding Ah receptor. Science 268, 722–726.

Gadepalli, V.S., Vaughan, C., Rao, R.R., 2013. Isolation and characterization of murine multipotent lung stem cells. Methods Mol. Biol. 962, 183–191.

Giangreco, A., Reynolds, S.D., Stripp, B.R., 2002. Terminal bronchioles harbor a unique airway stem cell population that localizes to the bronchoalveolar duct junction. Am. J. Pathol. 161, 173–182.

Giangreco, A., Arwert, E.N., Rosewell, I.R., Snyder, J., Watt, F.M., Stripp, B.R., 2009. Stem cells are dispensable for lung homeostasis but restore airways after injury. Proc. Natl. Acad. Sci. U. S. A. 106, 9286–9291.

Gomez-Duran, A., Carvajal-Gonzalez, J.M., Mulero-Navarro, S., Santiago-Josefat, B., Puga, A., Fernandez-Salguero, P.M., 2009. Fitting a xenobiotic receptor into cell homeostasis: how the dioxin receptor interacts with TGF beta signaling. Biochem. Pharmacol. 77, 700–712.

Gong, X., Sun, Z., Cui, D., Xu, X., Zhu, H., Wang, L., Qian, W., Han, X., 2014. Isolation and characterization of lung resident mesenchymal stem cells capable of differentiating into alveolar epithelial type II cells. Cell Biol. Int. 38, 405–411.

Hofsteen, P., Mehta, V., Kim, M.S., Peterson, R.E., Heideman, W., 2013. TCDD inhibits heart regeneration in adult zebrafish. Toxicol. Sci. 132, 211–221.

Hong, K.U., Reynolds, S.D., Watkins, S., Fuchs, E., Stripp, B.R., 2004a. Basal cells are a multipotent progenitor capable of renewing the bronchial epithelium. Am. J. Pathol. 164, 577–588.

Hong, K.U., Reynolds, S.D., Watkins, S., Fuchs, E., Stripp, B.R., 2004b. In vivo differentiation potential of tracheal basal cells: evidence for multipotent and unipotent subpopulations. Am. J. Physiol. Lung Cell Mol. Physiol. 286, L643–649.

Jackson, D.P., Li, H., Mitchell, K.A., Joshi, A.D., Elferink, C.J., 2014. Ah receptor-mediated suppression of liver regeneration through NC-XRE-driven p21Cip1 expression. Mol. Pharmacol. 85, 533–541.

Kim, C.F., Jackson, E.L., Woolfenden, A.E., Lawrence, S., Babar, I., Vogel, S., Crowley, D., Bronson, R.T., Jacks, T., 2005. Identification of bronchioalveolar stem cells in normal lung and lung cancer. Cell 121, 823–835.

Ko, C.I., Fan, Y., de Gannes, M., Wang, Q., Xia, Y., Puga, A., 2016. Repression of the aryl hydrocarbon receptor is required to maintain mitotic progression and prevent loss of pluripotency of embryonic stem cells. Stem Cells 34, 2825–2839.

Kotton, D.N., Morrisey, E.E., 2014. Lung regeneration: mechanisms, applications and emerging stem cell populations. Nat. Med. 20, 822–832.

Lahvis, G.P., Lindell, S.L., Thomas, R.S., McCuskey, R.S., Murphy, C., Glover, E., Bentz, M., Southard, J., Bradfield, C.A., 2000. Portosystemic shunting and persistent fetal vascular structures in aryl hydrocarbon receptor-deficient mice. Proc. Natl. Acad. Sci. U. S. A. 97, 10442–10447.

Lahvis, G.P., Pyzalski, R.W., Glover, E., Pitot, H.C., McElwee, M.K., Bradfield, C.A., 2005. The aryl hydrocarbon receptor is required for developmental closure of the ductus venosus in the neonatal mouse. Mol. Pharmacol. 67, 714–720.
Leeman, K.T., Fillmore, C.M., Kim, C.F., 2014. Lung stem and progenitor cells in tissue homeostasis and disease. Curr. Top. Dev. Biol. 107, 207–233.
Marlowe, J.L., Puga, A., 2005. Aryl hydrocarbon receptor, cell cycle regulation, toxicity, and tumorigenesis. J. Cell. Biochem. 96, 1174–1184.
Marlowe, J.L., Knudsen, E.S., Schwemberger, S., Puga, A., 2004. The aryl hydrocarbon receptor displaces p300 from E2F-dependent promoters and represses S phase-specific gene expression. J. Biol. Chem. 279, 29013–29022.
Mathew, L.K., Andreasen, E.A., Tanguay, R.L., 2006. Aryl hydrocarbon receptor activation inhibits regenerative growth. Mol. Pharmacol. 69, 257–265.
Mitchell, K.A., Lockhart, C.A., Huang, G., Elferink, C.J., 2006. Sustained aryl hydrocarbon receptor activity attenuates liver regeneration. Mol. Pharmacol. 70, 163–170.
Morales-Hernandez, A., Gonzalez-Rico, F.J., Roman, A.C., Rico-Leo, E., Alvarez-Barrientos, A., Sanchez, L., Macia, A., Heras, S.R., Garcia-Perez, J.L., Merino, J.M., Fernandez-Salguero, P.M., 2016. Alu retrotransposons promote differentiation of human carcinoma cells through the aryl hydrocarbon receptor. Nucleic Acids Res. 44, 4665–4683.
Mulero-Navarro, S., Fernandez-Salguero, P.M., 2016. New trends in aryl hydrocarbon receptor biology. Front Cell Dev. Biol. 4, 45.
Nakagawa, M., Yamanaka, S., 2010. Reprogramming of somatic cells to pluripotency. Adv. Exp. Med. Biol. 695, 215–224.
North, D.W., Abdo, K.M., Benson, J.M., Dahl, A.R., Morris, J.B., Renne, R., Witschi, H., 2008. A review of whole animal bioassays of the carcinogenic potential of naphthalene. Regul. Toxicol. Pharmacol. 51, S6–14.
O'Donnell, E.F., Saili, K.S., Koch, D.C., Kopparapu, P.R., Farrer, D., Bisson, W.H., Mathew, L.K., Sengupta, S., Kerkvliet, N.I., Tanguay, R.L., Kolluri, S.K., 2010. The anti-inflammatory drug leflunomide is an agonist of the aryl hydrocarbon receptor. PLoS One 5.
Pan, G., Li, J., Zhou, Y., Zheng, H., Pei, D., 2006. A negative feedback loop of transcription factors that controls stem cell pluripotency and self-renewal. FASEB J. 20, 1730–1732.
Peng, T., Frank, D.B., Kadzik, R.S., Morley, M.P., Rathi, K.S., Wang, T., Zhou, S., Cheng, L., Lu, M.M., Morrisey, E.E., 2015. Hedgehog actively maintains adult lung quiescence and regulates repair and regeneration. Nature 526, 578–582.
Pohjanvirta, R., 2012. The AH Receptor in Biology and Toxicology. 1st ed. John Wiley & Sons, New York.
Puga, A., Marlowe, J., Barnes, S., Chang, C.Y., Maier, A., Tan, Z., Kerzee, J.K., Chang, X., Strobeck, M., Knudsen, E.S., 2002. Role of the aryl hydrocarbon receptor in cell cycle regulation. Toxicology 181–182, 171–177.
Quintana, F.J., Basso, A.S., Iglesias, A.H., Korn, T., Farez, M.F., Bettelli, E., Caccamo, M., Oukka, M., Weiner, H.L., 2008. Control of T(reg) and T(H)17 cell differentiation by the aryl hydrocarbon receptor. Nature 453, 65–71.
Rawlins, E.L., Hogan, B.L., 2006. Epithelial stem cells of the lung: privileged few or opportunities for many? Development 133, 2455–2465.
Rawlins, E.L., Okubo, T., Xue, Y., Brass, D.M., Auten, R.L., Hasegawa, H., Wang, F., Hogan, B.L., 2009. The role of Scgb1a1+ Clara cells in the long-term maintenance and repair of lung airway, but not alveolar, epithelium. Cell Stem Cell 4, 525–534.
Reynolds, S.D., Giangreco, A., Power, J.H., Stripp, B.R., 2000. Neuroepithelial bodies of pulmonary airways serve as a reservoir of progenitor cells capable of epithelial regeneration. Am. J. Pathol. 156, 269–278.
Rico-Leo, E.M., Alvarez-Barrientos, A., Fernandez-Salguero, P.M., 2013. Dioxin receptor expression inhibits basal and transforming growth factor beta-induced epithelial-to-mesenchymal transition. J. Biol. Chem. 288, 7841–7856.
Rico-Leo, E.M., Moreno-Marin, N., Gonzalez-Rico, F.J., Barrasa, E., Ortega-Ferrusola, C., Martin-Munoz, P., Sanchez-Guardado, L.O., Llano, E., Alvarez-Barrientos, A., Infante-Campos, A., Catalina-Fernandez, I., Hidalgo-Sanchez, M., de Rooij, D.G., Pendas, A.M., Pena, F.J., Merino, J.M., Fernandez-Salguero, P.M., 2016. piRNA-associated proteins and retrotransposons are differentially expressed in murine testis and ovary of aryl hydrocarbon receptor deficient mice. Open Biol. 6, 160186.
Rock, J.R., Onaitis, M.W., Rawlins, E.L., Lu, Y., Clark, C.P., Xue, Y., Randell, S.H., Hogan, B.L., 2009. Basal cells as stem cells of the mouse trachea and human airway epithelium. Proc. Natl. Acad. Sci. U. S. A. 106, 12771–12775.
Rock, J.R., Gao, X., Xue, Y., Randell, S.H., Kong, Y.Y., Hogan, B.L., 2011. Notch-dependent differentiation of adult airway basal stem cells. Cell Stem Cell 8, 639–648.
Roman, A.C., Carvajal-Gonzalez, J.M., Rico-Leo, E.M., Fernandez-Salguero, P.M., 2009. Dioxin receptor deficiency impairs angiogenesis by a mechanism involving VEGF-A depletion in the endothelium and transforming growth factor-beta overexpression in the stroma. J. Biol. Chem. 284, 25135–25148.
Sauzeau, V., Carvajal-Gonzalez, J.M., Riolobos, A.S., Sevilla, M.A., Menacho-Marquez, M., Roman, A.C., Abad, A., Montero, M.J., Fernandez-Salguero, P., Bustelo, X.R., 2011. Transcriptional factor aryl hydrocarbon receptor (Ahr) controls cardiovascular and respiratory functions by regulating the expression of the Vav3 proto-oncogene. J. Biol. Chem. 286, 2896–2909.
Sharan, K., Mishra, J.S., Swarnkar, G., Siddiqui, J.A., Khan, K., Kumari, R., Rawat, P., Maurya, R., Sanyal, S., Chattopadhyay, N., 2011. A novel quercetin analogue from a medicinal plant promotes peak bone mass achievement and bone healing after injury and exerts an anabolic effect on osteoporotic bone: the role of aryl hydrocarbon receptor as a mediator of osteogenic action. J. Bone Miner. Res. 26, 2096–2111.
Song, H., Yao, E., Lin, C., Gacayan, R., Chen, M.H., Chuang, P.T., 2012. Functional characterization of pulmonary neuroendocrine cells in lung development, injury, and tumorigenesis. Proc. Natl. Acad. Sci. U. S. A. 109, 17531–17536.
Sutherland, K.M., Edwards, P.C., Combs, T.J., Van Winkle, L.S., 2012. Sex differences in the development of airway epithelial tolerance to naphthalene. Am. J. Physiol. Lung Cell Mol. Physiol. 302, L68–81.
Takahashi, K., Yamanaka, S., 2016. A decade of transcription factor-mediated reprogramming to pluripotency. Nat. Rev. Mol. Cell Biol. 17, 183–193.
Taub, R., 2004. Liver regeneration: from myth to mechanism. Nat. Rev. Mol. Cell Biol. 5, 836–847.
Teisanu, R.M., Lagasse, E., Whitesides, J.F., Stripp, B.R., 2009. Prospective isolation of bronchiolar stem cells based upon immunophenotypic and autofluorescence characteristics. Stem Cells 27, 612–622.
Veldhoen, M., Hirota, K., Westendorf, A.M., Buer, J., Dumoutier, L., Renauld, J.C., Stockinger, B., 2008. The aryl hydrocarbon receptor links TH17-cell-mediated autoimmunity to environmental toxins. Nature 453, 106–109.
Volckaert, T., De Langhe, S., 2014. Lung epithelial stem cells and their niches: Fgf10 takes center stage. Fibrogenesis Tissue Repair 7, 8.
Wang, Q., Kurita, H., Carreira, V., Ko, C.I., Fan, Y., Zhang, X., Biesiada, J., Medvedovic, M., Puga, A., 2016. Ah receptor activation by dioxin disrupts activin, BMP, and WNT signals during the early differentiation of mouse embryonic stem cells and inhibits cardiomyocyte functions. Toxicol. Sci. 149, 346–357.
Yamamoto, H., Yun, E.J., Gerber, H.P., Ferrara, N., Whitsett, J.A., Vu, T.H., 2007. Epithelial-vascular cross talk mediated by VEGF-A and HGF signaling directs primary septae formation during distal lung morphogenesis. Dev. Biol. 308, 44–53.
Yu, H., Du, Y., Zhang, X., Sun, Y., Li, S., Dou, Y., Li, Z., Yuan, H., Zhao, W., 2014. The aryl hydrocarbon receptor suppresses osteoblast proliferation and differentiation through the activation of the ERK signaling pathway. Toxicol. Appl. Pharmacol. 280, 502–510.